Measurement of the complex dielectric constant down to helium temperatures. II. Quasioptical technique from 0.03 to 1 THz

J. A. Reedijk, H. C. F. Martens, B. J. G. Smits, and H. B. Brom

Measurement of the complex dielectric constant down to helium temperatures. II. Quasioptical technique from 0.03 to 1 THz

J. A. Reedijk, H. C. F. Martens,[a] B. J. G. Smits, and H. B. Brom

Kamerlingh Onnes Laboratory, Leiden University, P.O. Box 9504, 2300 RA Leiden, The Netherlands

A quasioptical method is described that allows the determination of the complex dielectric constant almost continuously in the millimeter wave regime without the use of electrical contacts. The technique allows the dielectric properties of bulk samples (solids, powders, and liquids) and thin films (free standing or deposited on a substrate) to be measured with excellent absolute accuracy down to 2 K. © *2000 American Institute of Physics.* [S0034-6748(00)04902-9]

I. INTRODUCTION

As argued in the preceding article,[1] referred to as paper I, the frequency dependent dielectric response $\bar{\epsilon}$ of a material generally contains a wealth of information about the nature of carrier transport, localization of charge carriers, dipolar relaxation, etc. To obtain this information, it is essential that $\bar{\epsilon}$ is accurately measured over as broad a range in frequency as possible.

Microwave techniques, see paper I, are generally restricted on the high frequency side to approximately 20 GHz, above which coaxial lines and connectors start to show strong damping. Far-infrared detection methods[2,3] on the other hand are limited to the long wavelength side to about 5 cm^{-1} (150 GHz) due to the $\omega^{-1/2}$ dependence of thermal noise power.[3] The limitations of the above mentioned techniques thus leave a gap of approximately one frequency decade wide, where dielectric experiments cannot be performed by standard methods.

Shridar *et al.*[4] solved this problem by the use of complex impedance bridges. This technique is particularly well suited to measure the temperature and frequency dependence of needle-shaped samples, like quasi-one-dimensional materials. Here we present a quasioptical technique that overlaps in frequency with the end of the microwave regime as well as with the long wavelength side of the far-infrared spectrum and allows easy access of low temperatures. It provides a necessary tool to obtain a complete frequency scan of the dielectric function from low (Hz) to high (infrared) frequencies and is especially suited for films of, e.g., polymers and pellets of powders. The complex transmission through a sheet of material is measured in small frequency bands. Fitting the data to first principles formulas, the dielectric parameters follow directly from the experiments without further assumptions and without the use of Kramers-Kronig analysis.

II. EXPERIMENTAL SETUP

The quasioptical setup is schematically drawn in Fig. 1. A monochromatic signal with adjustable frequency (8–18

GHz) is produced by a local yttrium-iron-garnet (YIG) oscillator. At the sender horn (2), a harmonic generator creates the millimeter wave radiation (30–120 GHz), which is directed towards the sample by the horn antenna and focused by means of a polyethylene lens. At the sample spot, the material is placed at an oblique angle (usually 10°–15°). The transmitted radiation is again focused by a second lens onto the receiver horn (3). At this horn, the incoming radiation is mixed with a higher harmonic of a second YIG oscillator frequency, which is phase locked to the first YIG and operating at a slightly lower frequency. The resulting beat signal is returned to the ABmm oscillator/detector, where the amplitude and phase of the transmitted radiation are extracted.

For frequencies above 120 GHz the higher harmonics of the YIGs are insufficiently powerful in this case, a base frequency is created by an intense, external Gunn diode oscillator operating around 95 GHz, and multiplied by a number $N \leq 6$ by a special harmonic generator. Because the Gunn frequency is phase locked to the YIG oscillators, phase information is maintained, i.e., vector detection is possible up to 570 GHz. In principle, using a set of Gunn diodes operat-
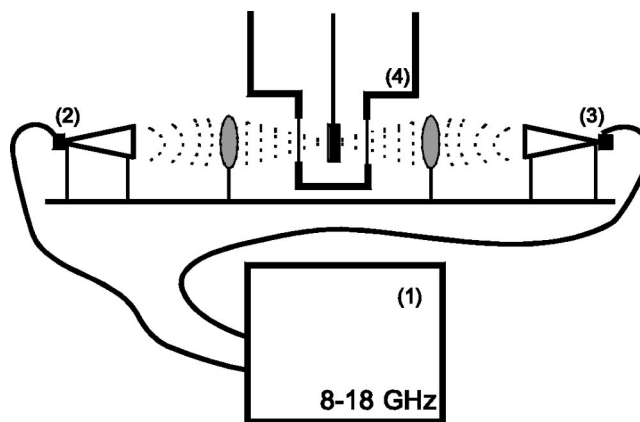

FIG. 1. Typical arrangement of a quasioptical setup, illustrated for an ABmm vector network analyzer. The frequency of the main frame (1) is variable between 8 and 18 GHz. Multiplication to higher harmonic frequencies occurs at the sender horns (2); at the receiver horn (3) a beat signal is generated, which is returned to (1). The sample is located in the tail of an optical cryostat (4) in the focus of two lenses.

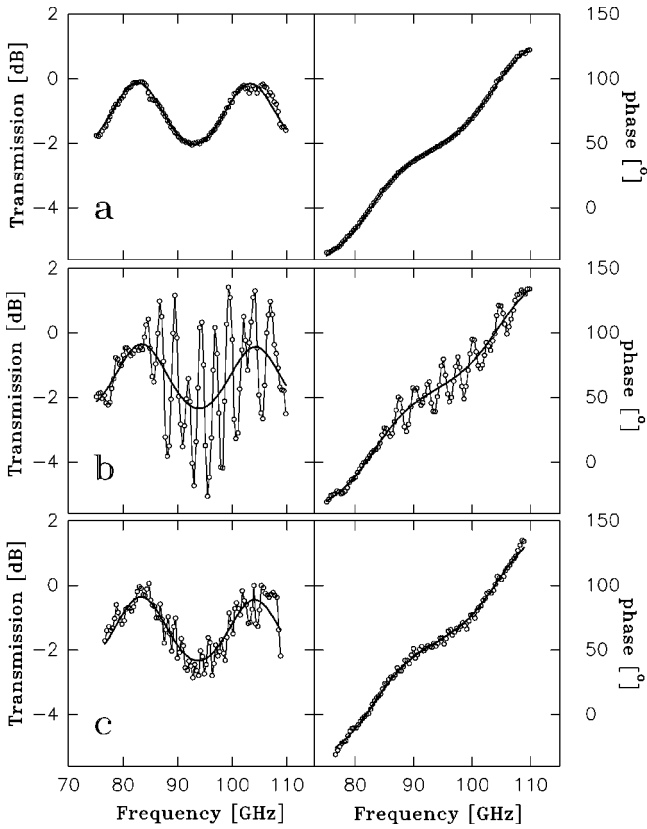[a]Electronic mail: martens@phys.leidenuniv.nl

FIG. 2. Frequency scan from 75–110 GHz of a quartz slab, fitted to Eq. (7). (a) Measurement outside the cryostat; (b) raw data of experiment inside the cryostat; (c) data of (b) after Fourier-spectrum manipulation; the fast oscillations observed in (b) are due to multiple reflections on the cryostat windows. The slow modulation is due to multiple reflections *within* the sample, which are incorporated in the transmission analysis. The χ^2 values of the fits are 3×10^{-2}, 3×10^{0}, and 4×10^{-1}, respectively.

ing at 110 GHz, frequencies up to 0.9 THz can be achieved.[5]

Experiments at reduced temperatures are performed using a modified Oxford Instruments optical cryostat [indicated by (4) in Fig. 1]. Because of the long wavelength of the GHz radiation (up to 1 cm), the cryostat windows were enlarged from 12 to 40 mm to minimize effects of scattering on the window edges. The sample space windows are made from 130 μm Kapton foils. The sample is cooled down to 4.2 K by flowing helium through the sample space. Temperatures between 2.0 and 4.2 K can be achieved by pumping the liquid helium filled sample space. Using a slidable and rotatable insert, the sample can be moved upwards to make a baseline measurement possible with the possibility of varying the angle of incidence.

III. CALCULATION OF TRANSMISSION

When a plane wave falls from medium 1 on a plane-parallel slab of material 2 of thickness d, generally the transmission through the slab is given by[6]

$$T = \frac{t_{12}t_{21}\exp[-\gamma_z d]}{1 - r_{21}^2 \exp[-2\gamma_z d]}, \tag{1}$$

where t_{ij} and r_{ij} are the transmission and reflection from

medium i to j, and γ_z is the component along the z axis, chosen normal to the slab, of the propagation constant in material 2.

Consider now a plane electromagnetic wave with propagation constant $\boldsymbol{\gamma}_0$ in air (medium 1), incident on nonmagnetic medium 2 with relative complex dielectric constant $\bar{\epsilon}_r = \epsilon' - i\epsilon''$. When the E field is polarized perpendicular to the plane formed by $\boldsymbol{\gamma}_0$ and the surface normal $\mathbf{n}$, the transmission is given by[6]

$$t_{12} = \frac{2\cos\theta}{\cos\theta + \sqrt{\bar{\epsilon}_r - \sin^2\theta}}, \tag{2}$$

where θ is the angle between $\boldsymbol{\gamma}_0$ and $\mathbf{n}$. The transmission and reflection of a plane wave in medium 2 incident on a boundary with air are given by

$$t_{21} = \frac{2\sqrt{\bar{\epsilon}_r - \sin^2\theta}}{\cos\theta + \sqrt{\bar{\epsilon}_r - \sin^2\theta}}, \tag{3}$$

$$r_{21} = \frac{\sqrt{\bar{\epsilon}_r - \sin^2\theta} - \cos\theta}{\cos\theta + \sqrt{\bar{\epsilon}_r - \sin^2\theta}}. \tag{4}$$

The complex nature of the amplitudes in Eqs. (2)–(4) implies the fact that the transmitted and reflected waves differ in phase from the incident wave.

The propagation constant in medium 2, $\boldsymbol{\gamma} = \boldsymbol{\alpha} + i\boldsymbol{\beta}$ deserves some attention, since the attenuation vector $\boldsymbol{\alpha}$ and the phase vector $\boldsymbol{\beta}$ are generally not parallel.[7] The z component of $\vec{\gamma}$ is given by $\gamma_z = \alpha + i\beta\cos\zeta$, where $\alpha = |\boldsymbol{\alpha}|$, $\beta = |\boldsymbol{\beta}|$, and $\boldsymbol{\alpha} \cdot \boldsymbol{\beta} = \alpha\beta\cos\zeta$. After some elementary manipulations, it is found[8] that $\alpha = -\omega/c \, \mathrm{Im}\sqrt{\bar{\epsilon}_r - \sin^2\theta}$ and $\beta\cos\zeta = \omega/c \, \mathrm{Re}\sqrt{\bar{\epsilon}_r - \sin^2\theta}$, so that we can write

$$\gamma_z = i\frac{\omega}{c}\sqrt{\bar{\epsilon}_r - \sin^2\theta}. \tag{5}$$

Combining Eqs. (1)–(5) leads to

$$T = \frac{4\gamma_z\gamma_{0z}\exp[-\gamma_z d]}{(\gamma_{0z} + \gamma_z)^2 - (\gamma_{0z} - \gamma_z)^2\exp[-2\gamma_z d]}, \tag{6}$$

where $\gamma_{0z} = i\omega/c \, \cos\theta$ is the z component of $\boldsymbol{\gamma}_0$. In every experiment, the measurement of the transmission of a material is directly preceded or followed by a similar measurement without the presence of the sample. Dividing the complex transmission data in principle leads to a canceling of all effects that are not due to the sample, apart from a phase shift of $\exp[-\gamma_{0z}d]$ due to the optical path of the removed sample; after the data are multiplied by this phase factor, they can be fitted to Eq. (6), thus allowing $\bar{\epsilon}$ to be directly extracted from the measurements.

One effect, that cannot be compensated for by a baseline measurement, is the transmission of radiation that is initially reflected by the sample, cryostat windows or receiver horn, but reflected again by one of these elements. This radiation, which will interfere with the transmitted signal, is different for sample and baseline measurements, since inserting a sample changes the optical path and hence the interference patterns. The resulting data [an example is plotted in Fig. 2(b)] show clear oscillations as a function of frequency,
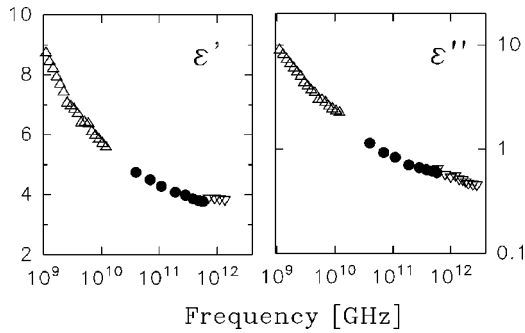
FIG. 3. Complex dielectric constant of a conducting carbon-black/polymer composite ($p = 1$ vol%) measured at seven frequency intervals between 30 and 600 GHz (filled circles). The open triangles represent data from open-ended coaxial and FTIR spectroscopic techniques, respectively.

which are eliminated using Fourier-spectrum manipulation. When l is the distance between reflecting elements, the oscillations in the frequency dependent transmission will have a period of c/l, giving a peak in the Fourier spectrum at $t = l/c$. Removing this peak and transforming the spectrum back [see Fig. 2(c)] leads to a considerable improvement of the data quality and hence of the fits giving ϵ' and ϵ''.

IV. EXAMPLES

A typical measurement is shown in Fig. 2(b); here the transmission of a quartz substrate mounted inside the cryostat is plotted (dots). The full lines represent fits to Eq. (6). The same data, after the Fourier-spectrum manipulation mentioned above, are shown in Fig. 2(c), together with the fits to Eq. (6). For comparison, transmission data on the same sample outside the cryostat are shown in Fig. 2(a), also with a corresponding fitting lines. The fit to the first data set yields $\epsilon' = 3.81 \pm 0.01$ and $\epsilon'' = 0.009 \pm 0.006$, the second data set gives $\epsilon' = 3.80 \pm 0.10$ and $\epsilon'' = 0.02 \pm 0.05$. In the third case, the dielectric parameters are $\epsilon' = 3.81 \pm 0.02$ and $\epsilon'' = 0.015 \pm 0.010$.

The room temperature dielectric function of a composite of carbon black dispersed into an insulating polymer matrix is shown in Fig. 3. The data taken in the range 30–600 GHz are seen to interpolate well between those taken with open-ended coaxial (up to 20 GHz) and Fourier-transform infrared (above 500 GHz) techniques.

In Fig. 4, the dielectric constant and conductivity at 475 GHz of a 1-μm-thin poly-aniline film close to the metal-insulator transition is shown as a function of temperature between 2 and 250 K. The conductivity σ' is related to the imaginary part of the dielectric function via $\sigma' = \omega \epsilon'' \epsilon_0$. In this plot, the measurement uncertainty is approximately given by the symbol size, $\Delta \epsilon' = 10$ and $\Delta \sigma' = 4$ S/cm at all temperatures.

When the number of charge carriers present in the studied material can be varied by means of an external signal, for instance via electrode injection or carrier excitation using light, an additional possibility of the experimental setup can be exploited. By modulating the carrier density and measuring the transmission on the appropriate side-band, the sensitivity can be easily increased by a factor 10^3. In Fig. 5, the transmission is plotted of a silicon slab irradiated by 2 eV
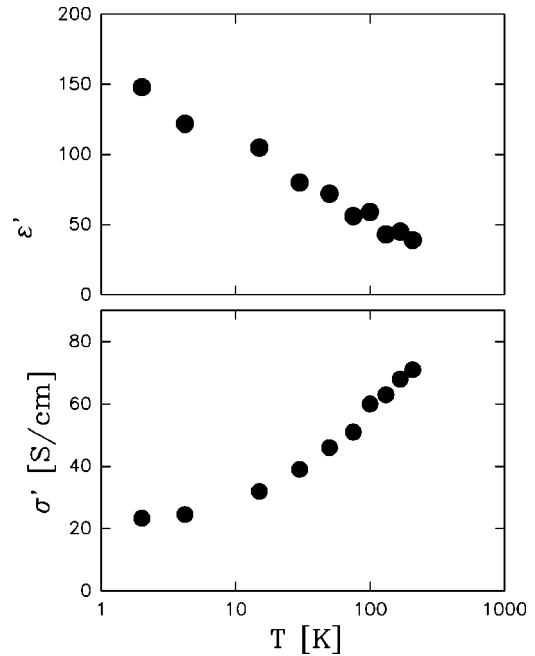

FIG. 4. The dielectric constant and conductivity at 475 GHz of a polyaniline film close to the metal-insulator transition, measured between 2 and 300 K.

light. Fitting the data to Eq. (7) leads to $\epsilon' = 11.4 \pm 0.1$ and $\sigma' = (0.0 \pm 0.1)$ S/m without light, and $\epsilon' = 11.2 \pm 0.1$ and $\sigma' = (12.6 \pm 0.2)$ S/m for the silicon slab irradiated with light.

V. DISCUSSION

A strong point of the quasioptical technique described here is the high accuracy with which the dielectric properties can be determined. Because the detection is phase sensitive, incoherent (i.e., thermal) noise is averaged out, and the measurement accuracy will be limited by other sources of error.

In the first place, the stability of the setup has to be considered. Because a frequency scan typically takes a time of the order of a minute, the setup has to be stable during several minutes to get reliable results. For the ABmm used here, typical figures for the drift in phase (ϕ) and amplitude (A) are $d\phi/dt \leq 0.5°/$min and $dA/dt \leq 0.02$ dB/min, respectively. The effects of drift are eliminated to first order by taking two baseline measurements, one before and one after the sample measurement, and averaging the results.

The fact, that the incoming waves are not truely plane, also forms a possible source of error. The radiation is created at the sender antenna, which is a point source and thus produces a spherical wave. This means that strictly speaking the transmission equation, Eq. (6), being only valid for plane incident waves, may not be used. However, when the distance between horns and sample is kept large (in our case it is always fixed at 40 cm, i.e., 50 to 1000 wavelengths), the wave front will be very close to being plane at the sample spot, thus resulting in negligible error.[6]

A more serious deviation from the ideal geometry is formed by the finite size of the sample, cryostat windows, and lenses; because of this, scattering on the edges of these elements can become important. This effect can be mini-
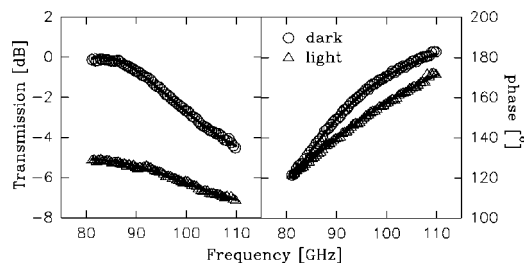
FIG. 5. Frequency scan between 80–110 GHz of a silicon slab, (a) without light and (b) irradiated with 2 eV light. The solid lines represent fits to Eq. (7).

mized by properly lining out the setup, so that the radiation is maximally focused on the sample spot. However, in practice an error of at least 1% remains, which rapidly becomes larger when the sample size decreases below approximately five wavelengths.

Another important source of error is the interference of directly transmitted and multiple reflected radiation, which was discussed above. To minimize this error, the frequency interval over which the transmission is continuously measured has to contain several oscillations due to this interference effect. In that case, a clear peak is present in the Fourier transform and the uncertainty due to interference effects can be kept below 2%. One might also reduce the interference by placing the sample at a small angle with the incoming wave, so that reflected radiation is coupled out of the system. For experiments inside the cryostat, this angle of incidence could be determined only within an accuracy of $2°$. Using not too large angles ($\theta \leq 15°$), the error in $\cos\theta$ and $\sin^2\theta$, which enter the transmission equations, remains below 1%.

Finally, the measurement accuracy is limited due to the occurance of coherent noise. When the sample thickness is much larger than the penetration depth δ of the studied material, i.e., when $d \gg \delta$, the power transmitted through the sample becomes very weak, and coherent noise becomes important. Since both the penetration depth $\delta \approx c/\sqrt{\sigma\omega/\epsilon_0}$, and the dynamic range decrease with frequency, the effects of coherent noise for weakly transmitting samples will be most apparent at high frequencies. Choosing the thickness small enough, the transmitted signal will sufficiently exceed the coherent noise level up to the highest frequencies.[9] In case the signal can be modulated, the influence of coherent noise can be completely eliminated by detection at the appropriate side band.

In summary, we have described a quasioptical technique which allows the accurate determination of dielectric properties down to low temperatures without the use of electrical contacts in the millimeter wavelength range, which is generally considered one of the hardest frequency regimes for performing reliable dielectric experiments. For the setup described here, the absolute value of the errors $\Delta\epsilon'/|\epsilon|$ and $\Delta\epsilon''/|\epsilon|$ typically are $\leq 2\%$ for room temperature measurements, and $\leq 4\%$ for experiments inside the cryostat, which is excellent compared to other experimental techniques in the microwave and far infrared regimes.

[1] H. C. F. Martens, J. A. Reedijk, and H. B. Brom, Rev. Sci. Instrum. **71**, 473 (2000).
[2] G. W. Chantry, *Long-Wave Optics* (Academic, London, 1984), pp. 294–398.
[3] D. Grischkowsky, S. Keiding, M. van Exter, and Ch. Fattinger, J. Opt. Soc. Am. B **7**, 2006 (1990).
[4] S. Shridar, D. Reagor, and G. Gruner, Rev. Sci. Instrum. **56**, 1946 (1985).
[5] P. Goy, Users Manual ABmm, Paris, 1992 (unpublished).
[6] R. M. Redheffer, in *Technique of Microwave Measurements*, edited by C. G. Montgomery (McGraw-Hill, New York, 1947), pp. 562–596.
[7] R. B. Adler, L. J. Chu, and R. M. Fano, *Electromagnetic Energy Transmission and Radiation* (Wiley, New York, 1960), pp. 402–448.
[8] J. A. Stratton, *Electromagnetic Theory* (McGraw-Hill, New York, 1941), pp. 482–505.
[9] In our case, the dynamic range varies from 110 dB at 30 GHz to 50 dB at 570 GHz (Ref. 5). Choosing $d \leq 5\delta$, measurements with an accuracy of a few percent can be made up to 570 GHz.